J. Chem. Sci., Vol. 117, No. 6, November 2005, pp. 657–661.

Influence of charged microenvironment on redox potential and diffusion coefficient of $[Fe_4S_4(SPh)_4](NBu_4)_2$ in DMF and inside CTAB film on electrode surface

RABEN CH ROY and DIGANTA KUMAR DAS*

Department of Chemistry, Gauhati University, Guwahati 781 014, India
e-mail: digkdas@yahoo.com

MS received 16 May 2005

Abstract. Redox potential of $[Fe_4S_4(SPh)_4]^{2-/3-}$, a model of the active centre of ferredoxin, in DMF solution shows a 90-mV positive shift, when the charged microenvironment provided by the surfactant is changed from negative to positive. Inside the positive surfactant film on GC electrode there is a 235-mV positive shift in redox potential compared to that in neutral DMF solution. Diffusion coefficient of the reduced cluster onto the electrode surface is also found to be 10^2 times greater in the presence of negative surfactant compared to that in positive surfactant.

Keywords. Ferredoxin; chronocoulometry; diffusion coefficient; redox potential; surfactant films.

1. Introduction

Iron sulphur proteins are ubiquitous in biochemistry, serving diverse roles ranging from simple biological electron transfer to chemical catalysis.[1] The electron carrying properties of these proteins are related to the ability of their iron sulphur active sites to exist in different oxidation levels interrelated by one-electron transfer reactions.

Various iron sulphur clusters with thiolate ligands have been synthesized as models of active sites of iron sulphur proteins.[2–7] Studies on the redox behaviour of these clusters surrounded by a hydrophobic environment are of biological significance.[3,8] The electrochemistry of these clusters has elucidated that synthetic water soluble Fe–S clusters in aqueous solution exhibit more positive redox potentials than water insoluble clusters in organic solvents.[5,9] Recent studies have shown that the microenvironment around the active centre plays a vital role in determining its redox potential.[10] The more positive redox potential of HiPIP as compared to ferredoxins is attributed to the fact that in HiPIP the Fe_4S_4 active centre is surrounded by several hydrophobic aromatic side chains that restrict solvent accessibility.[11] On the other hand, the active centre of ferredoxin is close to the protein surface and hence more exposed to the solvent. This is supported by the observation that in aqueous media the synthetic iron–sulphur cluster undergoes a 220-mV anodic shift in redox potential in the presence of bovine serum albumin.[9] Theoretical studies have also revealed that solvent exposure plays a major role in determining electrostatic environment and thereby the redox potential of the $[Fe_4S_4(SPh)_4]^{2-}$ cluster[12] (**I**).

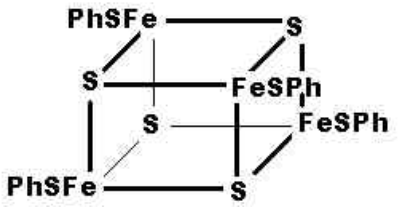

Structure of $[Fe_4S_4(SPh)_4]^{2-}$ (**I**).

Self-assembled monolayer (SAM) films on electrode surfaces have gained importance because of their applications in interfacial electron transfer, electrochemistry, biological membrane, catalysis etc.[13,14] It is well established that surfactants can be adsorbed on electrode surface to form a surfactant film.[15–17] The adsorption is through the hydrophobic surfactant tail on the electrode surface with the polar head group directed towards the bulk water phase.[18]

What is the effect of the hydrophobicity and nature of charge of the medium on the mid-point potential of

*For correspondence

the Fe–S cluster? In this paper we report the effect of charged surfactant molecules on the mid-point potential and diffusion co-efficient (on to the electrode surface) of the cluster $[Fe_4S_4(SPh)_4](NBu_4)_2$ in DMF. The mid-point potential of the cluster in the positive surfactant film on a glassy carbon electrode surface is also reported.

2. Materials and methods

$[Fe_4S_4(SPh)_4](NBu_4)_2$ is prepared as reported using a Schlenk line and found to show similar electronic spectra as reported earlier.[19] All the chemicals except triton X-100 (Sigma) are from Merck and used as received. The surfactants used are cetyltrimethylammonium bromide (CTAB), triton X-100 (TX-100) and sodiumdodecyl sulphate (SDS). These are cationic, neutral and anionic respectively. Surfactant solutions used are 3% (*w*/*v*) surfactant in dimethyl formamide (DMF). The DMF was distilled twice before use. The concentration of the cluster in different media is 1·94 mM (in CTAB), 0·82 mM (SDS) and 1·46 mM (TX-100).

BAS (Bioanalytical System, USA) 100 W electrochemical analyzer with a three-electrode cell assembly is used in our work. Cyclic voltammetry (CV) and Osteryoung square wave voltammetry (OSWV) are used to measure the redox potential under a blanket of dry nitrogen. The working electrode is platinum (Pt) and glassy carbon (GC) with the Ag–AgCl as reference electrode. Supporting electrolyte used is 0·1 M $NaClO_4$. For the OSWV experiments the square wave amplitude is 25 mV, the frequency 15 Hz and potential height for the base staircase wavefront 4 mV. Background voltammograms show that they are free from any redox interferences in the potential range of interest. The working electrode (WE) is cleaned before each run by polishing with 0·1 mM alumina using a BAS polishing kit followed by sonication.

Diffusion co-efficient of the cluster on to the electrode surface has been calculated using the Cottrell equation.[20] The area of the platinum electrode surface has been taken to be 0·025 cm^2.

2.1 *Preparation of film*

0·1 g CTAB and 0·1 g of the cluster is dissolved in 10 ml dichloromethane under a nitrogen environment. 0.5 *m*l of this solution is placed on the tip of glassy carbon electrode and allowed to evaporate under nitrogen environment. A piece of specially designed simple glassware is fabricated for this purpose (scheme 1), with an inlet and an outlet for nitrogen gas. The electrode is kept tip upwards in the vessel using a block of rubber. The mouth is then closed with a thin rubber stopper and nitrogen is passed for 5 min to flush out the air inside. The cluster solution is then placed on the tip of the electrode through the rubber stopper using a Hamilton syringe, while passing the nitrogen gas. The nitrogen gas is allowed to pass for ≈ 30 min so that the solvent completely evaporates from the electrode tip and a film is formed. Electrochemical experiments are performed by immersing the tip of this electrode into de-oxygenated Tris buffer (pH = 7·0) containing 0·1 M $NaNO_3$ as supporting electrolyte.

3. Results and discussions

Reversible cyclic voltammogram was observed for the cluster $[Fe_4S_4(SPh)_4](NBu_4)_2$ in DMF with mid-point potential value –990 mV vs Ag–AgCl as reference. This mid-point potential value was confirmed by OSWV measurements (table 1). This mid-point potential value is in close agreement with the reported mid-point potential value of the cluster for 2-/3-redox couples in DMF[+], thus confirming the formation of the cluster and the redox couple involved as 2-/3-.

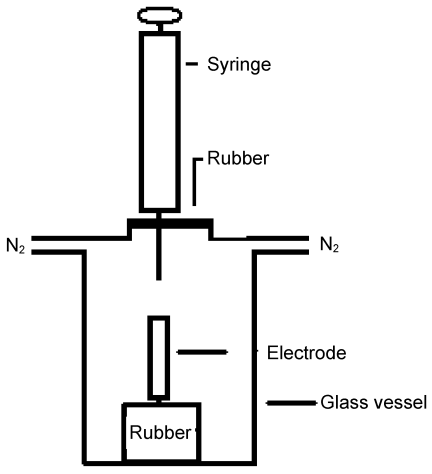

Scheme 1

[+]The redox potential, –990 mV vs Ag–AgCl, when converted with respect to saturated calomel electrode (SCE) as reference becomes –1037 mV and the reported redox potential due to the 2-/3-redox couple of the cluster, measured by polarography, is –1039 mV versus SCE[20]

Figure 1 shows the cyclic voltammogram of the cluster in CTAB solution in DMF. The redox potential is found to be –930 ± 5 mV with ΔEp = 97 mV (table 1). This redox potential value is further confirmed by OSWV experiments (table 1). The cluster is found to give reversible cyclic voltammogram in TX-100 in different scan rates (figure 2) with –965 ± 5 mV as redox potential. The plot of cathodic and anodic current vs square root of scan rate is linear (not shown). In SDS also, a reversible cyclic voltammogram is obtained with redox potential value –1020 ± 5 mV. OSWV experiment of the cluster in SDS gives the redox potential as –1022 (figure 3, table 1).

Thus, in the presence of neutral TX-100 surfactant molecules in DMF the redox potential of the cluster shows a positive shift of 25 mV due to the increased hydrophobicity of the medium. When cationic CTAB molecules are present in the vicnity of the cluster, compared to pure DMF, the mid-point potential of the cluster becomes 65 mV more positive. Here, both the increased hydrophobicity and electrostatic interactions may be the operative factors. The cluster in cationic CTAB is likely to be in the reduced 3-state making the reduction process easier and hence a positive shift in redox potential takes place. In anionic SDS, the redox potential is 35 mV negative than that in pure DMF. The cluster should be relatively more

Table 1. Electrochemical results of $[Fe_4S_4(SPh)_4]^{2-/3-}$ in different media.

WE = GCE, RE = Ag–AgCl (3N NaCl). D_o is the diffuson co-efficient of $[Fe_4S_4(SPh)_4]^{2-}$ onto GC electrode surface calculated using Cottrell equation from the slope of charge vs time$^{1/2}$ plots obtained from chronocoulometric experiments.

	E (mV)			
Medium	CV	OSWV	ΔE (mV)	D_o (cm^2 s^{-1})
DMF	–990	–992	90	–
CTAB/DMF	–930	–932	97	$0{\cdot}24 \times 10^{-8}$
TX-100/DMF	–965	–965	159	$0{\cdot}29 \times 10^{-6}$
SDS/DMF	–1020	–1022	125	$7{\cdot}84 \times 10^{-6}$
CTAB-film	–755	–753	380	–

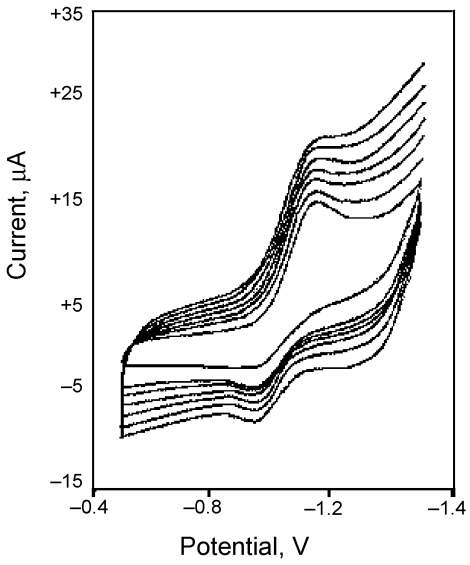

Figure 2. Cyclic voltammogram of 1·46 mM $[Fe_4S_4(SPh)_4]^{2-/3-}$ in 3% (*w*/*v*) TX-100 at scan rates 50, 70, 80, 90, 100, 110 and 120 mV s^{-1} in increasing order of current. WE = platinum, RE = Ag–AgCl (3 M NaCl).

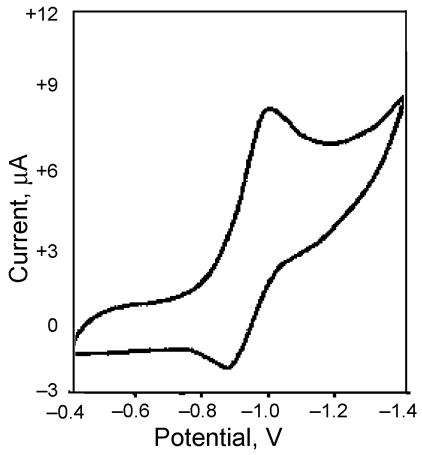

Figure 1. Cyclic voltammogram of 1·94 mM $[Fe_4S_4(SPh)_4]^{2-/3-}$ in 3% (*w*/*v*) CTAB in DMF. WE = platinum, RE = Ag–AgCl (3 M NaCl).

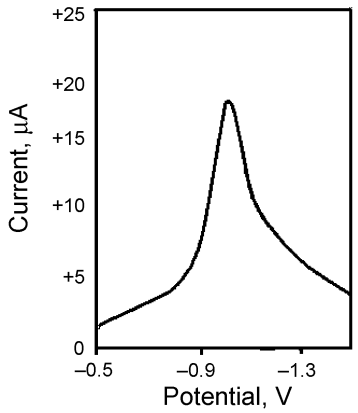

Figure 3. Osteryoung square wave voltammogram of 0·82 mM $[Fe_4S_4(SPh)_4]^{2-/3-}$ in 3% (*w*/*v*) SDS in DMF. WE = platinum, RE = Ag–AgCl (3 M NaCl).

stable in the 2-state over the 3-state, making reduction relatively difficult and hence a negative shift in mid-point potential. This electrostatic effect overcomes the positive shift due to the increased hydrophobicity of the medium by SDS molecules.

Figure 4 shows the cyclic voltammogram of the cluster in CTAB film on a glassy carbon (GC) electrode surface in Tris buffer (pH = 7·0). The redox potential value is found to be –755 mV vs Ag–AgCl (table 1) with ΔEp = 380 mV. This redox potential value is confirmed by OSWV measurement (figure 5). Thus in positive CTAB films the mid-point potential of the cluster is 235 mV more positive compared to that in DMF. Compared to DMF solution, in the film the positive charges are localized and is in greater proximity to the cluster which probably leads to the large positive shift in the redox potential of the cluster.

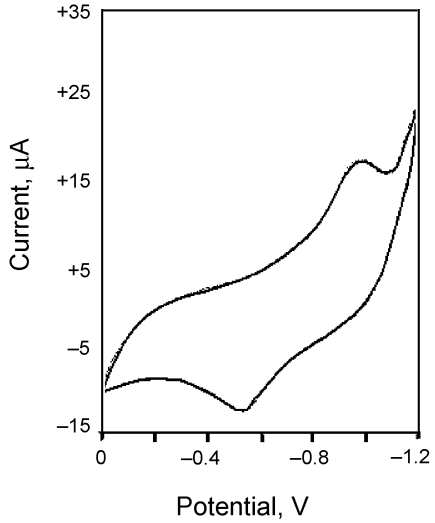

Figure 4. Cyclic voltammogram of $[Fe_4S_4(SPh)_4]^{2-/3-}$ in CTAB film on GC electrode surface in Tris buffer (pH = 7·0), RE = Ag–AgCl (3 M NaCl).

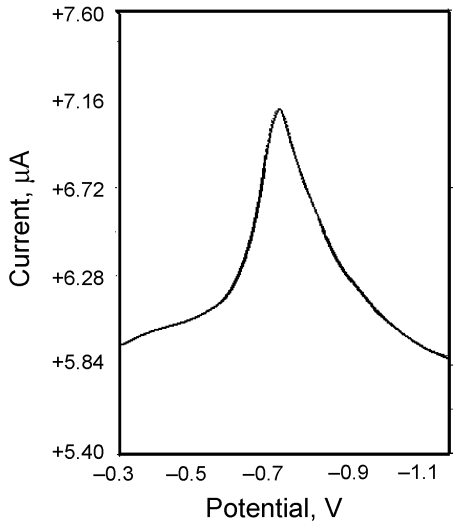

Figure 5. Osteryoung square wave voltammogram of $[Fe_4S_4(SPh)_4]^{2-/3-}$ in CTAB film on GC electrode surface in Tris buffer (pH = 7·0), RE = Ag–AgCl (3 M NaCl).

The double potential step chronocoulometric study is done for the cluster over the entire surfactant medium and CTAB film using a 250 mV pulse for 25 m s. The charge vs time and charge vs $(time)^{1/2}$ response is shown in figure 6 for the cluster in SDS solution. The charge vs $(time)^{1/2}$ plots are found to be linear, and for the reverse step the intercept is found to be 6·2 *m*A (SDS), 1·1 *m*A (CTAB), 2·2 *m*A (TX-100) and 31·4 *m*A (CTAB-Film). The diffusion co-efficients of the cluster onto the electrode surface in reduced state are $0{\cdot}24 \times 10^{-8}$, $0{\cdot}29 \times 10^{-6}$ and $7{\cdot}84 \times 10^{-6}$ $cm^2\ s^{-1}$ in CTAB, TX-100 and SDS in DMF medium. Thus the diffusion co-efficient is lowest in CTAB and of the order of 10^2 higher in SDS and TX-100. Electrostatic attraction between the negative charge of the cluster and the positive polar heads of the CTAB molecules is probably responsible for the slow diffusion of the cluster into the electrode surface in the case of the CTAB solution. On the other hand, the electrostatic repulsion between the negative cluster and negative polar head groups of the SDS molecules helps diffusion. The diffusion co-efficient and amount adsorbed could not be calculated for the cluster inside the CTAB film due to our inability to measure the thickness of the film and hence the concentration of the cluster inside the film.

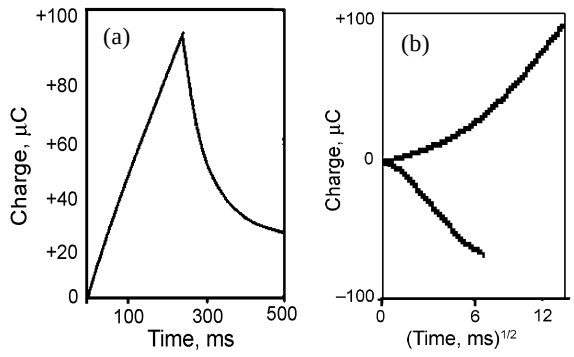

Figure 6. (**a**) Charge vs time response of double potential step chronocoulometry of $[Fe_4S_4(SPh)_4]^{2-/3-}$ in 3% (*w*/*v*) SDS. WE = platinum, RE = Ag–AgCl (3 M NaCl). (**b**) The Anson plot is obtained as the output from a BAS 100W electrochemical analyzer.

Thus we have shown that the redox potential of the cluster $[Fe_4S_4(SPh)_4]^{2-/3-}$ is significantly influenced by the nature of the charge around the cluster. As the environment changes from negative charge to positive, the redox potential shows a positive shift in the order SDS < DMF < TX-100 < CTAB. The net change in redox potential when the charged environment is changed from positive to negative is 85 mV. In films the effect of charge on redox potential is more effective as confirmed by the fact that CTAB-film imparts a 180 mV positive shift.

Acknowledgement

The authors thank the University Grants Commission, New Delhi for financial support.

References

1. Kennedy M L and Gibney B R 2002 *J. Am. Chem. Soc.* **124** 6826
2. Dukes G R and Holm R H 1975 *J. Am. Chem. Soc.* **97** 528
3. Holm R H 1977 *Acc. Chem. Res*. **10** 427
4. Nakamoto M, Tanaka K and Tanaka T 1986 *J. Chem. Soc., Chem. Commun*. 1669
5. Nakamoto M, Tanaka K and Tanaka T 1988 *Bull. Chem. Soc. Japan* **61** 4099
6. Okuno Y, Uoto K, Yonemitsu O and Tomohiro T 1987 *J. Chem. Soc., Chem. Commun.* 1018
7. Johnson R E, Papaefthymiou G C, Frenkel R B and Holm R H 1983 *J. Am. Chem. Soc.* **105** 7280
8. Evans M C W 1982 In *Iron sulphur proteins* (ed.) T G Spiro (New York: Wiley) p. 249
9. Odell B and Geary P J 1984 *J Chem. Soc., Dalton Trans*. 29
10. Backes G, Mino Y, Loehr T M, Meyer T E, Cusanovich M A, Sweeney W V, Adman E T and Loehr J S 1991 *J. Am. Chem. Soc.* **113** 2055
11. Duderstadt R E, Brereton P S, Adams M W W and Johnson M K 1999 *FEBS Lett.* **454** 21
12. Stephens P J, Jolie D R and Warshel A 1996 *Chem. Rev.* 1996
13. Caldwell W B, Campbell D J, Chen K, Herr B R, Mirkin C A, Malik A, Durbin M K, Dutta P and Huang K G 1995 *J. Am. Chem. Soc*. **117** 6071
14. Nuzzo R G and Allara D L 1983 *J. Am. Chem. Soc*. **105** 4481
15. Lyones M E G, Breen W and Carridy I 1991 *J. Chem. Soc., Faraday Trans.* **87** 113
16. Attwood D and Florence A T 1983 *Surfactant systems – Their chemistry, pharmacy and biology* (London: Chapman & Hall) ch. 1
17. Roy R C, Bhattacharjya R and Das D K 2004 *Indian J. Chem*. **A43** 1689
18. Wen X-lin, Han Z-Xu, Ricker A and Liu Z-Li 1997 *J. Chem. Res*. (*S*) 108
19. De Pamphilis B V, Averill B A, Herskovitz T, Que L and Holm R H 1974 *J. Am. Chem. Soc.* **96** 4159
20. Bard A J and Faukner L R 1980 *Electrochemical methods: Fundamentals and applications* (New York: Wiley) ch. 12, p. 535